Carbon nanotubes as nanoelectromechanical systems

S. Sapmaz, Ya. M. Blanter, L. Gurevich, and H. S. J. van der Zant
Department of NanoScience and DIMES, Delft University of Technology, Lorentzweg 1, 2628 CJ Delft, The Netherlands
(Received 19 November 2002; revised manuscript received 17 March 2003; published 20 June 2003)

We theoretically study the interplay between electrical and mechanical properties of suspended, doubly clamped carbon nanotubes in which charging effects dominate. In this geometry, the capacitance between the nanotube and the gate(s) depends on the distance between them. This dependence modifies the usual Coulomb models and we show that it needs to be incorporated to capture the physics of the problem correctly. We find that the tube position changes in discrete steps every time an electron tunnels onto it. Edges of Coulomb diamonds acquire a (small) curvature. We also show that bistability in the tube position occurs and that tunneling of an electron onto the tube drastically modifies the quantized eigenmodes of the tube. Experimental verification of these predictions is possible in suspended tubes of sub-micron length.

DOI: 10.1103/PhysRevB.67.235414 PACS number(s): 73.63.Nm, 46.70.Hg, 62.25.+g, 73.23.Hk

I. INTRODUCTION

Nanoelectromechanical systems (NEMS) convert electrical current into mechanical motion on a nanoscale and vice versa. These systems can be viewed as the successors[1] of microelectromechanical devices (MEMS), which operate at a micron scale and are found in commercial applications. An improved performance is expected from NEM devices due to their small sizes, and higher eigenfrequencies. M(N)EMS have already been used for high-precision measurements of force,[2] electric charge,[3] the thermal conductance quantum,[4] and the Casimir force.[5] From a fundamental point of view, NEM physics is an unexplored field in which new phenomena are likely to be found. Examples include tunneling through moving barriers,[6] additional sources of noise,[7] and shuttling mechanism for transport.[8–10]

Studies with NEMS have mostly been performed in devices made with silicon technology. Carbon nanotubes provide an interesting alternative because of their superior mechanical properties. These have already been implemented as nanotweezers,[11,12] as switches in a random access memory device,[13] or as nanoscale actuators.[14] In addition, recent theoretical calculations show that carbon nanotubes can also be used as nanoelectromechanical switches[15,16] or as gigahertz oscillators.[17]

In this paper, we study theoretically nanoelectromechanical effects in doubly clamped suspended carbon nanotubes. Doubly clamped suspended single-wall and multiwall carbon nanotubes have been previously fabricated, and their transport,[18–21] acoustoelectric,[22] thermal,[23] and elastic[24] properties have been measured. We consider a single-wall carbon nanotube (SWNT) in which Coulomb-blockade effects dominate transport, and demonstrate that a gate manipulates the tube in an effective way. The applied gate voltage bends the tube, changes the stress, and thus influences the electric and mechanical properties.

This paper is organized as follows. The following section describes the model with inclusion of the influence of initial stress and thermal fluctuations. We concentrate on the case where the junction capacitances are zero so that analytical expressions are obtained. Section III describes the influence of nanoelectromechanical effects on Coulomb blockade and shows that intrinsic bistability occurs when the tube is strained. Section IV discusses the eigenmodes and the influence on the initial strain on them. In Sec. V, junction capacitances are no longer neglected and we also show the effect of a nonuniform charge distribution. We end with some remarks on the limitations of our model.

II. DISPLACEMENT, STRESS, AND ENERGY

A. Equilibrium position

We consider a SWNT (modeled as a rod of length L along the x axis), freely suspended between source and drain electrodes, in the vicinity of a gate (see Fig. 1). The nanotube is attached to the electrodes via tunneling contacts. An electrostatic force (gate voltage) bends the tube; the deviation from a straight line is denoted by $z(x)$ with $0<x<L$. The elastic energy of the bent tube is[25]

$$W_{el}[z(x)]=\int_0^L dx\left\{\frac{EI}{2}z''^2+\left[\frac{T_0}{2}+\frac{ES}{8L}\int_0^L z'^2dx\right]z'^2\right\}, \tag{1}$$

where E, $I=\pi r^4/4$, and $S=\pi r^2$ are the elastic modulus, the inertia moment, and the cross section, respectively. Here, r is the (external) radius of the tube. The first term in Eq. (1) is the energy of an unstressed bent rod; other two terms describe the effect of the stress force $\tilde{T}=T_0+T$. Here, T_0 is the residual stress which may result, e.g., from the fabrication, and the induced stress T is due to the elongation of the tube caused by the gate voltage,

$$T=\frac{ES}{2L}\int_0^L z'^2dx. \tag{2}$$

To write down the electrostatic energy, we denote the capacitances of the barriers connecting the nanotube with the source and drain as C_L and C_R, respectively (see Fig. 1). The capacitance to the gate per unit length is $c(z)$. Approximating the gate by an infinite plane at a distance R from the nanotube, we obtain

 ©2003 The American Physical Society

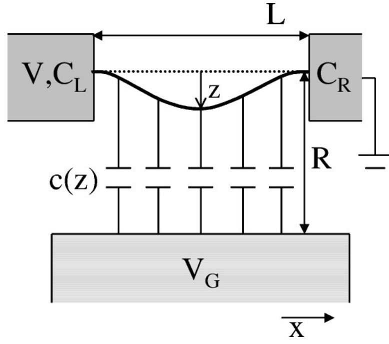

FIG. 1. A schematic drawing of a suspended nanotube capacitively coupled to a gate and clamped on both sides to metal pads that serve as tunnel contacts. A voltage V is applied to the left pad.

$$c(z)=\frac{1}{2\ln\frac{2(R-z)}{r}}\approx\frac{1}{2\ln\frac{2R}{r}}+\frac{z(x)}{2R\ln^2\frac{2R}{r}}, \tag{3}$$

where the Taylor expansion restricts validity to $z\ll R$. In this limit, van der Waals forces between the nanotube and the substrate can be neglected. The electrostatic energy of the system reads

$$W_{est}[z(x)] = \frac{(ne)^2-2ne(C_LV+C_GV_G)}{2(C_L+C_R+C_G)} - \frac{C_L(C_R+C_G)V^2+C_G(C_L+C_R)V_G^2-2C_LC_GVV_G}{2(C_L+C_R+C_G)}, \tag{4}$$

where V and V_G are the potentials of the source and the gate, respectively (the drain potential is set to zero), ne is the (quantized) excess charge on the nanotube, and for a uniform charge distribution the capacitance to the gate equals

$$C_G=\int_0^L c[z(x)]dx.$$

Note that the last term in Eq. (4) depends on the tube displacement and thus on the number of electrons. Therefore, it can not be omitted as in the standard Coulomb-blockade treatment that replaces this term by a constant making W_{est} a periodic function of gate voltage.

In the following, we concentrate on the analytically tractable case $C_L, C_R=0$. The general case is considered in Sec. V. For a moment, we also assume $T_0=0$. In this situation, the expression for the electrostatic energy simplifies to

$$W_{est}[z(x)]=\frac{(ne)^2}{2C_G[z]}-neV_G \approx \frac{(ne)^2\ln\frac{2R}{r}}{L}-\frac{(ne)^2}{L^2R}\int_0^L z(x)dx-neV_G. \tag{5}$$

Minimizing the energy,

$$W_n[z(x)]=W_{el}[z(x)]+W_{est}[z(x)],$$

with respect to z, one finds the equation determining the tube position,[25]

$$IEz''''-Tz''=K_0\equiv\frac{(ne)^2}{L^2R}, \tag{6}$$

where K_0 is the electrostatic force per unit length, which we approximate by a constant. Higher-order terms are small for $z\ll R$. To solve Eq. (6), we have to assume that the stress force T is constant, and find it later from the self-consistent condition [Eq. (2)].

The solution of Eq. (6) with the appropriate boundary conditions [for the doubly-clamped rod, $z(0)=z(L)=z'(0)=z'(L)=0$] has the form

$$z_n(x)=\frac{K_0L}{2T\xi}\left[\frac{\sinh\xi L}{\cosh\xi L-1}(\cosh\xi x-1)-\sinh\xi x+\xi x-\xi\frac{x^2}{L}\right],\quad \xi=\sqrt{\frac{T}{EI}}. \tag{7}$$

Substituting this into Eq. (2), a relation between the stress T and the external force K_0 is obtained. In the limiting cases, it reads

$$T=\begin{cases}K_0^2L^6S/(60480EI^2), & T\ll EI/L^2\\ (ES/24)^{1/3}(K_0L)^{2/3}, & T\gg EI/L^2.\end{cases} \tag{8}$$

The first line corresponds to weak bending of the tube. The energy associated with the bending exceeds the energy of the stress. Generally, it is realized for $z\lesssim r$. The second line describes strong bending, when the tube displacement is large $(r<z\ll R,L)$.

For the displacement of the tube center $z_n^{max}=z_n(L/2)$, we find

$$z_n^{max}=0.003\,\frac{(ne)^2L^2}{Er^4R},\quad T\ll\frac{EI}{L^2}\left(n\ll\frac{Er^5R}{e^2L^2}\right)$$

$$z_n^{max}=0.24\,\frac{(ne)^{2/3}L^{2/3}}{E^{1/3}r^{2/3}R^{1/3}},\quad T\gg\frac{EI}{L^2}\left(n\gg\frac{Er^5R}{e^2L^2}\right). \tag{9}$$

For a SWNT with $r=0.65$ nm, $E=1.25$ TPa, $L=500$ nm, and $R=100$ nm (to be referred to as the E nanotube), the crossover from weak to strong bending, $T\sim EI/L^2$, occurs already at $n\sim 5-10$. In the strong-bending regime, the displacement of the E nanotube is (in nanometers) $z_n^{max}=0.24n^{2/3}$. Note that this regime is not accessible with state-of-the-art silicon submicron devices, which are always in the weak-bending limit.

B. Charge and energy

For comparison with experiments, we have to relate the charge ne to the gate voltage by minimizing the energy. The expression for the energy (elastic plus electrostatic) of the tube at equilibrium in the limiting cases reads

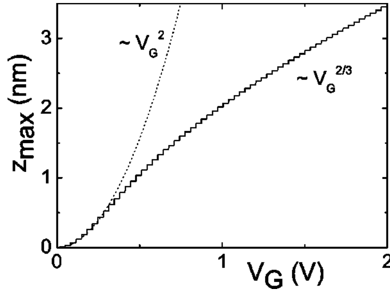

FIG. 2. Calculated displacement as a function of gate voltage for the E nanotube: $r=0.65$ nm, $E=1.25$ TPa, $L=500$ nm, and $R=100$ nm. At $V_G\approx 0.5$ V, there is a crossover from weak bending with a V_G^2 dependence to strong bending with a $V_G^{2/3}$ dependence.

$$W_n^{eq}\equiv W_{st}-\delta W=\frac{(ne)^2}{L}\ln\frac{2R}{r}-neV_G -\begin{cases}0.0009(ne)^4L/(Er^4R^2), & T\ll EI/L^2\\ 0.08(ne)^{8/3}/(Er^2R^4L)^{1/3}, & T\gg EI/L^2.\end{cases} \tag{10}$$

The first two terms represent the electrostatic energy of a straight tube, and the third one is due to the elastic degrees of freedom (stress, bending, and change of C_G due to displacement). This nonlinear, *nanomechanical term* is typically a small correction. For the E nanotube, it becomes of the same order as W_{st} if $n\sim 3000$ in which case Eq. (3) is not valid anymore. The negative sign of the nanomechanical contribution is easily understood. As the gate voltage changes, the movable tube adjusts not only its charge but also its position, which leads to a lower energy as compared to the fixed-position system.

The value of n which minimizes the energy is

$$n=\mathrm{Int}\left(\frac{V_GL}{2e\ln(2R/r)}+\frac{1}{2}+\delta n\right),$$

with Int denoting the integer part of the expression. The small correction δn in the strong-bending regime is proportional to $V_G^{5/3}$. Thus, the tube displacement z_{max} changes in discrete steps when V_G is varied as shown in Fig. 2. The envelope is proportional to V_G^2 (weak bending) or $V_G^{2/3}$ (strong bending). In the absence of charging effects and tension, the displacement is given by the dashed line as previously found in simulations of Ref. 15.

C. Thermal fluctuations

The preceding considerations are restricted to the case of zero temperature. To understand the role of the temperature, we now evaluate the effect of thermal fluctuations on the equilibrium position of the tube.

The variance of the position of the tube center at a given charge n can be generally represented as a functional integral:

$$\mathrm{var}\,z_n\equiv\langle[z(L/2)-z_n(L/2)]^2\rangle =\frac{\partial^2}{\partial J^2}\int Dz(x)\exp[-W_n[z]/k_B\Theta+Jz(L/2)]|_{J=0} \times\left[\int Dz(x)\exp(-W_n[z]/k_B\Theta)\right]^{-1}, \tag{11}$$

where Θ is the temperature. Except for $n=0$, the functional integral in Eq. (11) is not Gaussian and has to be linearized around the equilibrium solution $z_n(x)$, Eq. (7). The remaining Gaussian integral can be calculated, and we arrive at

$$\mathrm{var}\,z_n=k_B\Theta\,\zeta(L/2), \tag{12}$$

where $\zeta(x)$ solves the equation

$$EI\zeta''''-\frac{ES}{2L}\int z_n'^2dx\,\zeta''-\frac{ES}{L}z_n''\int\zeta' z_n'dx=\delta(x-L/2). \tag{13}$$

In the two limiting cases of weak and strong bendings, the solution of Eq. (13) yields

$$\mathrm{var}\,z_n=\begin{cases}k_B\Theta L^3/192EI, & n=0\\ k_B\Theta L/8T, & n\gg Er^5R/e^2L^2,\end{cases} \tag{14}$$

where the stress T is still given by the lower line of Eq. (8). Thus, the fluctuations in the tube position are expected to grow linearly with temperature. However, their magnitude is small. For the E nanotube, at 100 K the fluctuations in the $n=0$ state are of the order of 0.1 nm, and at least an order of magnitude less in the strong-bending regime.

In the calculations, we have assumed that the charge ne is a fixed quantity. Close to the degeneracy points $W_n^{eq}=W_{n+1}^{eq}$, thermal fluctuations may induce switching between the states with charges ne and $(n+1)e$, in this case Eq. (14) is no longer valid. However, the range of voltages, where switching is important, is narrow.

III. COULOMB EFFECTS AND BISTABILITY

A. Coulomb blockade

Since the nanotube is attached to the electrodes by tunneling contacts, it is in the Coulomb-blockade regime. We define the energy to add the nth electron to the tube as $S_n=W_n-W_{n-1}$. Then, if the nanotube contains $n>0$ electrons, the conditions that current cannot flow (is Coulomb blocked) are $S_n<0$, $eV<S_{n+1}$. In quantum dots, S_n depends linearly on the bias V and gate V_g voltages. Thus, in the V_G-V plane, regions with zero current are confined within Coulomb diamonds, that are identical diamond-shape structures repeating along the V_G axis.

In a suspended carbon nanotube, in addition to the purely Coulomb energy, we also have the nanomechanical corrections. Generally, these corrections make the relations between V and V_G, which describe the boundaries of Coulomb-blockade regions, nonlinear. Consequently, the Coulomb "diamonds" in suspended nanotubes are not diamonds any more, but instead have a curvilinear shape (with

the exception of the case $C_L = C_R = 0$). Their size is also not the same and decreases with $|V_G|$. Thus, the mechanical degrees of freedom *affect* the Coulomb-blockade diamonds. However, since these effects originate from the nanomechanical term, which is typically a small correction, its influence on Coulomb diamonds is small as well. For the E nanotube, these effects do not exceed several percent for typical gate voltages.

B. Two-gate setup and bistability

To demonstrate that the nanomechanical effects cannot generally be omitted, we consider a suspended tube symmetrically placed in between two gates and show below that bistability in the tube position occurs.[26]

Figure 1 again presents the schematic setup, but the suspended tube is placed between two gates, labeled up (U) and down (D). Since up and down capacitances are connected in parallel, their sum $C_G = C_U + C_D$ matters. Assuming that the distance of the straight tube to both gates is the same, we write

$$C_{U,D} = \int_0^L \frac{dx}{2 \ln \frac{2(R \mp z)}{r}}. \tag{15}$$

Expanding this for $z \ll R$ and calculating the electrostatic force, we arrive at an equation similar to Eq. (6), with a constant force K_0 that is replaced by γz, where

$$\gamma = \frac{(ne)^2(\ln 2R/r + 2)}{2L^2 R^2 \ln 2R/r}.$$

We now solve this equation in the strong-bending regime. For this purpose[25] we disregard the term IEz'''', and use the boundary conditions $z(0) = z(L) = 0$. Multiple solutions emerge; the ones with the lowest energy are

$$z = \pm \frac{2L^2}{\pi^2} \sqrt{\frac{\gamma}{ES}} \sin \frac{\pi x}{L}. \tag{16}$$

Thus, the tube in the strong-bending regime can oscillate between the two symmetric positions. This creates a basis for observation of quantum effects, as discussed in Ref. 26. We emphasize once again that within this model, the multistability is due to the charging of the tube in combination with the nonlinearity.

IV. EIGENMODES

The eigenfrequency of a particular eigenmode is an important, directly measurable[22] property. In future experiments on suspended tubes, we expect that the eigenmodes influence tunneling ("phonon-assisted tunneling") in a similar way as observed for a single C_{60} molecule.[10] Below, we demonstrate that the effect of the electrostatic interactions on the elastic properties (specifically, eigenfrequencies) is strong and changes the behavior qualitatively.

To find the eigenmodes, we apply a gate voltage with a large dc (single gate) and a small ac component. The displacement $z(x,t)$ is time dependent, which provides an external force $-\rho S \ddot{z}$ to Eq. (6), where ρ equals 1.35 g/cm^3. Equation (6) must be solved first with a constant stress, and then the stress is found self-consistently. The tube displacement has a small ac component δz on top of a large static one. The self-consistency procedure is essentially the same and again leads to Eq. (8). Thus, the dc component of the gate voltage determines the stress T and it therefore controls the eigenmodes.

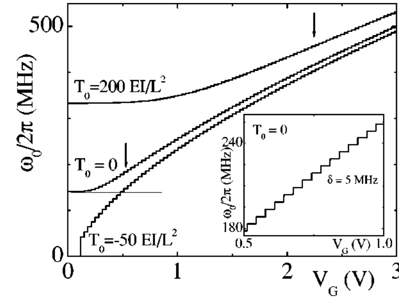

FIG. 3. Gate voltage dependence of the frequency ω_0 of the fundamental mode for three different values of the residual stress. Numbers are taken for the E nanotube (see Fig. 2). The fundamental mode of an unstressed tube is 140 MHz (thin horizontal line). The inset is an enlargement of the $T_0 = 0$ curve of the main figure showing stepwise increases of ω_0 whenever an additional electron tunnels onto the tube.

The frequencies of the (transverse) eigenmodes are found from the requirement that the equation

$$IE\,\delta z'''' - T\,\delta z'' - \rho S \omega^2 \delta z = 0 \tag{17}$$

with the boundary condition $\delta z(0) = \delta z(L) = \delta z'(0) = \delta z'(L) = 0$ has a nonzero solution. This yields the following equation for the frequency ω,

$$\cosh y_1 \cos y_2 - \frac{1}{2} \frac{y_1^2 - y_2^2}{y_1 y_2} \sinh y_1 \sin y_2 = 1$$

$$y_{1,2} = \frac{L}{\sqrt{2}} (\sqrt{\xi^4 + 4\lambda^2} \pm \xi^2)^{1/2}, \quad \lambda = \sqrt{\frac{\rho S}{EI}} \omega. \tag{18}$$

In the following, we restrict ourselves to the fundamental (lowest frequency) eigenmode ω_0. In the limiting cases, the solutions of Eq. (18) are

$$\omega_0 = \sqrt{\frac{EI}{\rho S}} \begin{cases} 22.38 L^{-2} + 0.28 \xi^2, & \xi L \ll 1 \\ \pi \xi L^{-1} + 2\pi L^{-2}, & \xi L \gg 1. \end{cases} \tag{19}$$

The second terms on the right-hand side represent small corrections to the first ones.

The frequency dependence $\omega_0 \propto L^{-2}$ is associated with a loose string, while $\omega_0 \propto L^{-1}$ means that the string is tied like in a guitar. Our results show that the behavior of the tube crosses over from "loose" to "tied" as V_G increases. For the fundamental mode, the crossover occurs at $\xi L \sim 1$, corresponding to the crossover from weak to strong bending. The middle curve in Fig. 3 shows the frequency of the fundamen-

tal mode as a function of gate voltage (zero residual stress). The arrow denotes the cross over from weak to strong bending.

The gate voltage dependence of the frequency is a stepwise function, as shown in the inset of Fig. 3. Steps occur whenever an additional electron tunnels onto the tube. For the E nanotube, their height is ~ 5 MHz, which is measurable. Note that the present submicron silicon devices are always in the weak-bending regime so that corrections due to the second term in Eq. (19) are too small to be measured. Furthermore, one should realize that frequency quantization is only observable if the frequency itself is greater than the inverse tunneling time for electrons.

We now consider the effect of a residual stress ($T_0 \neq 0$). First, we obtain the stress by solving Eqs. (2) and (6) (in the latter, T is replaced by $T+T_0$). In particular, for a negative stress $T+T_0<0$, $T_0 \sim -EI/L^2$, Eq. (2) acquires several solutions. This signals *Euler instability*: the tube bends in the absence of an external force.

If the residual stress is large, $T_0 \gg EI/L^2$, the tube always acts like a tied string (upper curve in Fig. 3). The frequency depends weakly on V_G for low voltages, and above $T \sim T_0$ (denoted with the arrow) grows with an envelope $\propto V_G^{2/3}$. For negative T_0, the picture is qualitatively different (lower curve in Fig. 3). Whereas for large gate voltages the envelope is still proportional to $V_G^{2/3}$, the frequency dives below the value for an unstressed tube $[22.38(EI/\rho S)^{1/2}L^{-2}$, represented by the thin solid line in Fig. 3], when the overall stress becomes negative. It further drops to zero at the Euler instability threshold.

The qualitative difference between the various regimes means that by measuring the gate voltage dependence of ω_0, one can determine the sign of T_0 and get a quantitative estimate. On the other side, the gate effect can be used to tune the eigenfrequencies. We also mention that in the absence of charging effects, the steps vanish but the overall shape of the curves in Fig. 3 remains the same.

V. RELAXING THE APPROXIMATIONS

While considering equilibrium displacement and eigenmodes of the nanotube, we made a number of simplifying approximations. In this section, we consider two of them—disregarding the capacitances $C_{L,R}$ and uniform distribution of the charge—and show that relaxing these approximations affects the above results quantitatively, but not qualitatively.

In this section, we consider the case of zero residual stress $T_0=0$.

A. Finite capacitances to the leads

We now relax the limitation $C_L, C_R=0$. For the general case, Eq. (6) still holds, however, the force K_0 must be adjusted,

$$K_0=\frac{1}{L^2R}\frac{C_0^2}{(C_0+C_R+C_L)^2}[ne+(C_L+C_R)V_G-C_LV]^2, \tag{20}$$

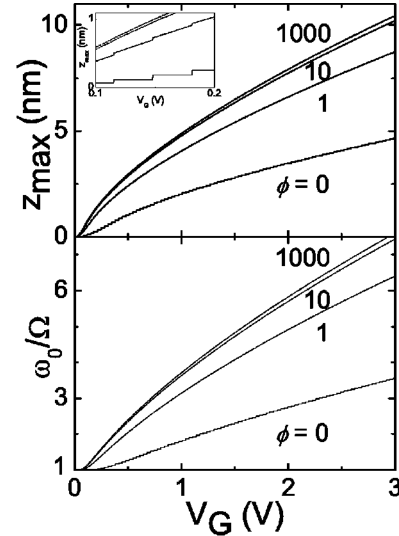

FIG. 4. Above: Displacement as a function of gate voltage for the E nanotube with finite capacitances to the leads. The four curves correspond to different values of the parameter ϕ, defined as $C_L = C_R = \phi C_G$. The inset is an enlargement of the main figure. Below: The frequency of the fundamental mode normalized to the fundamental frequency of an unstressed tube $\Omega = 22.38L^{-2}(EI/\rho S)^{1/2} = 141$ MHz for the same parameters as above.

where $C_0 = L/(2\ln 2R/r)$ is the capacitance of the straight nanotube to the gate. The results of the numerical solutions for the displacement and the frequency of the fundamental mode are plotted in Fig. 4. For simplicity, we have taken $C_L = C_R = \phi C_G$; the four curves correspond to different values of the parameter ϕ. The curves with $\phi=0$ are the same as the ones in Figs. 2 and 3.

The plots demonstrate that the qualitative picture remains the same if we include finite capacitances to the leads. The steps observed for $\phi=0$ become skewed with the increase of C_L and C_R (see inset of Fig. 4). At a certain ϕ these disappear. For $\phi>10$ the plots are, on the scale presented, the same.

B. Nonuniform charge distribution

Above, we have assumed a uniform charge distribution along the nanotube. Rather than trying to analyze the effect in general, we consider the opposite situation when the excess charge is concentrated at one point (to be more precise, in a concise region of the tube radius r), which may represent, for instance, a pinning center. This center is placed in the middle of the nanotube. Though we believe that the charge distribution in suspended nanotubes is closer to uniform, this situation applies to a suspended quantum dot as realized recently.[27]

The gate-charge capacitance C_G in this geometry is

$$C=\frac{1}{\frac{1}{r}-\frac{1}{2R}}, \tag{21}$$

and we proceed to obtain the equations of motion

$$IEz'''' - Tz'' = F\delta\left(x - \frac{L}{2}\right), \quad F \equiv \frac{(ne)^2}{4R^2}, \tag{22}$$

where we again set $C_L = C_R = 0$.

The solution with the same boundary conditions as previously, $z(0)=z(L)=z'(0)=z'(L)=0$, and with z, z', and z'' all continuous at $x=L/2$, is

$$z(x) = \frac{F}{2EI\xi^3}\left\{\tanh\frac{\xi L}{2}[\cosh\xi x - 1] - \sinh\xi x + \xi x\right\} \tag{23}$$

for $0<x<L/2$. For $L/2<x<L$, the coordinate x should be replaced by $(L-x)$ because $z(x)=z(L-x)$. As before, $\xi = (T/EI)^{1/2}$ and Eq. (2) is used to obtain the stress self-consistently,

$$T = \begin{cases} F^2L^4S/(30720EI^2), & T \ll EI/L^2 \\ (1/2)(ESF^2)^{1/3}, & T \gg EI/L^2. \end{cases} \tag{24}$$

Consider now the strong-bending regime and compare the results for the stress T_u for the uniform [lower line of Eq. (8)] and T_n for the concentrated [lower line of Eq. (24)] charge distributions,

$$T_n = T_u\left(\frac{\sqrt{3}L}{4R}\right)^{2/3}. \tag{25}$$

For $L \gg R$, we formally have $T_n \gg T_u$. This means that for the same gate voltage, more stress is induced at the nanotube if the charge is concentrated at one point. Also, the displacement of the tube is greater in the concentrated case,

$$z^n_{max} = 0.87\left(\frac{L}{R}\right)^{1/3} z^u_{max}.$$

Thus, if the charge distribution is concentrated, NEMS are "more effective" than for the uniform charge. For the E nanotube, the ratio of nonuniform to uniform maximal displacement is 1.49. The difference between uniform and nonuniform charge distributions is illustrated in Fig. 5.

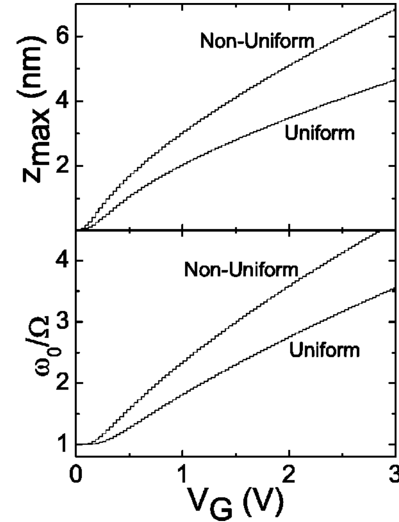

FIG. 5. Displacement of the center of the E nanotube (above) and the frequency of the fundamental eigenmode (below) for uniform charge distribution and for the case that the charge is concentrated at one point. Ω is the fundamental frequency of an unstressed tube.

VI. DISCUSSION

The presented model is simplified in many respects. Mechanical degrees of freedom are introduced via classical theory of elasticity: The nanotube (modeled by a rod) is considered as incompressible and without internal structure. This is justified, since so far the theory of elasticity has described all existing experiments on carbon nanotubes well. For SWNT's it has also been supported by simulations (Ref. 15). Creation of defects in SWNT starts at deformations of the order of 10%. For larger deformations (see, e.g., Ref. 28), we expect strong deviations from the behavior we describe, but this typically lies outside our applicability range $z \ll R$. We have neglected damping, which is also expected to originate from the creation of the defects and to be irrelevant in this range. We also disregarded quantum effects (cotunneling and finite spacing of quantum levels of electrons in the tube). These issues need to be clarified for a detailed comparison with the experimental data, and will be a subject of future research.

Our main result is that the nanotube can be manipulated by the gate voltage, which determines its deformation and stress, and modifies the eigenmodes. Though the eigenmodes of nanotube ropes have been measured in Ref. 22 three years ago, the *strain dependence* of the eigenmodes was only recently reported in Ref. 29, which was published after this manuscript had been submitted for publication. Reference 29 demonstrates this effect for singly-clamped multiwall carbon nanotubes. We expect that our predictions will soon be tested in experiments on doubly clamped SWNTs.

We also mention one more paper published after the submission of our manuscript, Ref. 27, which shows measurements on a suspended quantum dot. Though the focus of our study was on carbon nanotubes, all the calculations can be immediately applied to this case as well.

ACKNOWLEDGMENTS

We thank Yu. V. Nazarov, P. Jarillo-Herrero, L. P. Kouwenhoven, and C. Dekker for discussions. This work was supported by the Netherlands Foundation for Fundamental Research on Matter (FOM) and ERATO. H.S.Jv.d.Z. was supported by the Dutch Royal Academy of Arts and Sciences (KNAW).

[1] For an overview, see M. Roukes, Phys. World **14** (2), 25 (2001).
[2] T.D. Stowe, K. Yasumura, T.W. Kenny, D. Botkin, K. Wago, and D. Rugar, Appl. Phys. Lett. **71**, 288 (1997).
[3] A.N. Cleland and M.L. Roukes, Nature (London) **392**, 160 (1998).
[4] K. Schwab, E.A. Henriksen, J.M. Worlock, and M.L. Roukes, Nature (London) **404**, 974 (2000).
[5] H.B. Chan, V.A. Aksyuk, R.N. Kleiman, D.J. Bishop, and F. Capasso, Science **291**, 1941 (2001).
[6] N.F. Schwabe, A.N. Cleland, M.C. Cross, and M.L. Roukes, Phys. Rev. B **52**, 12911 (1995).
[7] A.V. Shytov, L.S. Levitov, and C.W.J. Beenakker, Phys. Rev. Lett. **88**, 228303 (2002).
[8] L.Y. Gorelik, A. Isacsson, M.V. Voinova, B. Kasemo, R.I. Shekhter, and M. Jonson, Phys. Rev. Lett. **80**, 4526 (1998); C. Weiss and W. Zwerger, Europhys. Lett. **47**, 97 (1999); T. Nord, L.Y. Gorelik, R.I. Shekhter, and M. Jonson, Phys. Rev. B **65**, 165312 (2002).
[9] M.T. Tuominen, R.V. Krotkov, and M.L. Breuer, Phys. Rev. Lett. **83**, 3025 (1999); A. Erbe, C. Weiss, W. Zwerger, and R.H. Blick, *ibid.* **87**, 096106 (2001).
[10] H. Park, J. Park, A.K.L. Lim, E.H. Anderson, A.P. Alivisatos, and P.L. McEuen, Nature (London) **407**, 57 (2000).
[11] P. Kim and C.M. Lieber, Science **286**, 2148 (1999).
[12] S. Akita, Y. Nakayama, S. Mizooka, Y. Takano, T. Okawa, Y. Miyatake, S. Yamanaka, M. Tsuji, and T. Nosaka, Appl. Phys. Lett. **79**, 1691 (2001).
[13] T. Rueckes, K. Kim, E. Joselevich, G.Y. Tseng, C.-L. Cheung, and C.M. Lieber, Science **289**, 94 (2000).
[14] See, e.g., R.H. Baughman, C. Cui, A.A. Zakhidov, Z. Iqbal, J.N. Barisci, G.M. Spinks, G.G. Wallace, A. Mazzoldi, D. De Rossi, A.G. Rinzler, O. Jaschinski, S. Roth, and M. Kertesz, Science **284**, 1340 (1999).
[15] M. Desquesnes, S.V. Rotkin, and N.R. Aluru, Nanotechnology **13**, 120 (2002).
[16] J.M. Kinaret, T. Nord, and S. Viefers, Appl. Phys. Lett. **82**, 1287 (2003).
[17] Q. Zheng and Q. Jiang, Phys. Rev. Lett. **88**, 045503 (2002); S.B. Legoas, V.R. Coluci, S.F. Braga, P.Z. Coura, S.O. Dantas, and D.S. Galvão, *ibid.* **90**, 055504 (2003).
[18] T.W. Tombler, C. Zhou, L. Alexseyev, J. Kong, H. Dai, L. Liu, C.S. Jayanthi, M. Tang, and S.-Y. Wu, Nature (London) **405**, 769 (2000).
[19] J. Nygård and D.H. Cobden, Appl. Phys. Lett. **79**, 4216 (2001).
[20] P.A. Williams, S.J. Papadakis, M.R. Falvo, A.M. Patel, M. Sinclair, A. Seeger, A. Helser, R.M. Taylor II, S. Washburn, and R. Superfine, Appl. Phys. Lett. **80**, 2574 (2002).
[21] N.R. Franklin, Q. Wang, T.W. Tombler, A. Javey, M. Shim, and H. Dai, Appl. Phys. Lett. **81**, 913 (2002).
[22] B. Reulet, A.Yu. Kasumov, M. Kociak, R. Deblock, I.I. Khodos, Yu.B. Gorbatov, V.T. Volkov, C. Journet, and H. Bouchiat, Phys. Rev. Lett. **85**, 2829 (2000).
[23] P. Kim, L. Shi, A. Majumdar, and P.L. McEuen, Phys. Rev. Lett. **87**, 215502 (2001).
[24] G.-T. Kim, G. Gu, U. Waizmann, and S. Roth, Appl. Phys. Lett. **80**, 1815 (2002).
[25] L.D. Landau and E.M. Lifshits, *Theory of Elasticity* (Pergamon, Oxford, 1986).
[26] S.M. Carr, W.E. Lawrence, and M.N. Wybourne, Phys. Rev. B **64**, 220101 (2001) discuss a bistability as a result of *externally applied* negative residual tension. We emphasize that in our case it appears for an arbitrary residual tension, in the regime when the charging effects drive the tube into the strong-bending regime.
[27] E.M. Höhberger, R.H. Blick, F.W. Beil, W. Wegscheider, M. Bichler, and J.P. Kotthaus, Physica E (Amsterdam) **12**, 487 (2002); E.M. Höhberger *et al.*, (unpublished).
[28] B.I. Yakobson, C.J. Brabec, and J. Bernholc, Phys. Rev. Lett. **76**, 2511 (1996).
[29] S.T. Purcell, P. Vincent, C. Journet, and Vu Thien Binh, Phys. Rev. Lett. **89**, 276103 (2002).